# Toroidal Dipolar Response in a Metamaterial

T. Kaelberer,[1] V. A. Fedotov,[1]* N. Papasimakis,[1] D. P. Tsai,[2,3] N. I. Zheludev[1]*

Toroidal multipoles are fundamental electromagnetic excitations different from those associated with the familiar charge and magnetic multipoles. They have been held responsible for parity violation in nuclear and particle physics, but direct evidence of their existence in classical electrodynamics has remained elusive. We report on the observation of a resonant electromagnetic response in an artificially engineered medium, or metamaterial, that cannot be attributed to magnetic or charge multipoles and can only be explained by the existence of a toroidal dipole. Our direct experimental evidence of the toroidal response brings attention to the often ignored electromagnetic interactions involving toroidal multipoles, which could be present in naturally occurring systems, especially at the macromolecule level, where toroidal symmetry is ubiquitous.

An electric (or charge) dipole results from a separation of positive and negative charges, whereas a magnetic dipole is produced by the closed circulation of an electric current (Fig. 1, A and B). Mathematically they appear in the series expansion (known as the multipole expansion) of an electromagnetic potential generated by a distribution of charges and currents (*1*, *2*). The toroidal dipole, an elusive counterpart of the charge and magnetic dipoles, is produced by currents flowing on the surface of a torus along its meridians (Fig. 1C). Toroidal dipoles were first considered by Zel'dovich in 1957 [who called them anapoles (*3*)] and have already been acknowledged in nuclear and particle physics [see (*4*, *5*) and references within]. First-principles calculations have revealed the existence of toroidal dipoles for certain molecular structures (*6*) and ferroelectric systems (*7*).

Toroidal dipoles and higher toroidal multipoles are the subject of growing interest because of their unusual electromagnetic properties. In particular, it has been shown that the strength of their interaction with electric and magnetic fields depends not on the strength of the fields, but rather on their time derivatives (*8*). It has also been suggested that nonstationary charge-current configurations involving toroidal multipoles could produce oscillating and propagating vector potential in the absence of electromagnetic fields (*9*, *10*). Media containing molecules with elements of toroidal symmetry could rotate the polarization of light (*11*) or could exhibit a negative index of refraction (*12*). Afanasiev (*13*) claimed that interactions between electrical currents producing toroidal multipoles would violate Newton's Third Law, which requires that the mutual forces between two interacting bodies are equal, opposite, and colinear. Furthermore, a material with domains of toroidal polarization is expected to have different optical properties along opposite directions (*14*).

Toroidal multipoles are not a part of the standard multipole expansion (*15*). The electromagnetic fields generated by an arbitrary system of nonstationary charges and currents are usually presented as a sum of contributions from two families of conventional elementary radiation sources: the magnetic and electric dynamic multipoles (*1*, *2*). In a spherical coordinate system, magnetic multipoles are defined by transversal components of oscillating current density (currents flowing on the surface of a sphere), whereas electric multipoles are attributed to oscillating charge density (charge multipoles). Radiating fields, however, also contain contributions from oscillating radial components of the current density. These radial components of the current density lead to the existence of the independent family of dynamic toroidal multipoles that are different from the magnetic and charge multipoles (*16*–*18*).

The most primitive member of the toroidal multipole family is the toroidal dipole **T** (*15*). It is created by poloidal currents (currents flowing on the surface of a torus along its meridians), but can be equivalently represented by a set of magnetic dipoles **m** arranged head-to-tail along a loop (Fig. 1C) (*15*). The toroidal dipole points outward along the symmetry axis of the torus. Toroidal coils and molecular structures alike could also display toroidal dipole moments (*6*, *17*). The electromagnetic manifestations of the toroidal dipole, however, are usually masked by much stronger effects due to charge and magnetic multipoles, making observations of the toroidal response extremely challenging (*14*, *19*, *20*).

We demonstrate a classical system in which the electromagnetic response is directly related to the resonant excitation of the toroidal dipole. The resonant toroidal response has been observed in a "metamaterial slab," a two-dimensional array of artificially engineered electromagnetic scatterers of toroidal symmetry. Metamaterials enable us to access novel and exotic electromagnetic phenomena not found in nature (such as negative refraction and cloaking) by controlling the symmetry and character of the response through artificial structuring on a subwavelength scale. To emphasize the toroidal dipolar response, we have designed a metamolecule, the elementary building block of our metamaterial, where both the electric and magnetic dipole moments induced by an incident electromagnetic wave (as well as higher multipoles) are substantially suppressed while the toroidal response is spectrally isolated and resonantly enhanced to a detectable level.

We depart from the obvious toroidal solenoid-like wire configuration, as it would also support a strong magnetic dipole moment because of the helical nature of its windings (*13*). Our toroidal metamolecule is composed of four rectangular, electrically disconnected metallic wire loops ($a \times h$) embedded into a low-loss dielectric slab of overall size $d \times d \times h$. The loops are located in two mutually orthogonal planes and separated by a distance $r$ (Fig. 2A). The intersection of the planes gives the axis of the toroidal structure (parallel to the $z$ axis). All wire loops have identical splits $g$, which are located either on the top or bottom sides of the slab such that the entire metamolecule has an inversion center $C$ located on the axis of the structure (Fig. 2A). The metamolecule is placed in a rectangular unit cell $d \times d \times s$, which is periodically translated along $y$ and $z$ axes to form a metamaterial slab.

The structure of our metamolecule ensures some distinct electromagnetic properties. Apart from supporting a magnetic dipole mode, now routinely observed in other metamaterials (*21*), it supports a dominant mode of a toroidal dipole nature. Excitations of both modes are manifested as resonant features ***I*** and ***II*** in the metamaterial's transmission and reflection spectra, which were simulated and measured for an electromagnetic wave polarized along the $z$ axis (Fig. 3, A and B). The resonances result from the circular currents induced by the incident wave in all four loops of

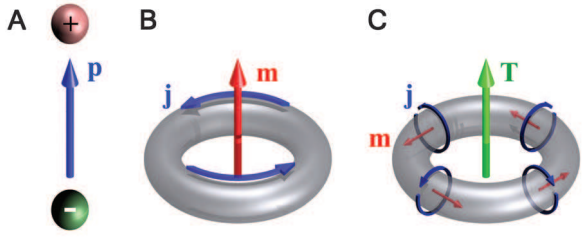


**Fig. 1.** (**A**) A pair of charges of opposite signs creates an electric (charge) dipole **p**. (**B**) A current **j** flowing along a loop produces a magnetic dipole **m**. (**C**) Currents flowing on a surface of a torus along its meridians (poloidal currents) generate a toroidal dipole **T**. The toroidal dipole can also be represented as a closed loop of magnetic dipoles arranged head-to-tail.

[1]Optoelectronics Research Centre and Centre for Photonic Metamaterials, University of Southampton, Southampton SO17 1BJ, UK. [2]Department of Physics, National Taiwan University, Taipei 10617, Taiwan. [3]Instrument Technology Research Center, National Applied Research Laboratories, Hsinchu 300, Taiwan.

*To whom correspondence should be addressed. E-mail: vaf@orc.soton.ac.uk (V.A.F.); niz@orc.soton.ac.uk (N.I.Z.); Web: www.nanophotonics.org.uk

the metamolecule. For *z*-polarization, these currents cannot be excited by the electric component of the wave, as it is orthogonal to the split of the loops. Correspondingly, the *z*-component of the electric dipole moment of the system $P_z$ is suppressed for both resonances. The metamolecule interacts with the magnetic part of the wave, which drives circular currents in accordance with Faraday's law of induction. When passing through the metamaterial slab, the wave reaches the front and rear pairs of the loops of the metamolecule with a phase delay. Thus, the magnetic field at the loops can be decomposed into parallel (in-phase) and antiparallel (antiphase) components. At resonance ***I*** the metamolecule interacts with the in-phase components of the magnetic field. The induced magnetic dipoles of all four loops **m** point in the same direction, producing a nonzero component of the metamolecule's net magnetic dipole moment $M_y$ parallel to the driving magnetic field (Fig. 2B), which reveals the magnetic origin of the resonance. By contrast, at resonance ***II*** the metamolecule couples to the antiphase components of the magnetic field and the individual magnetic moments induced in the front and rear pairs of the loops are directed oppositely, forming a head-to-tail configuration (Fig. 2C). Such a head-to-tail configuration of the individual magnetic moments **m** has a nonzero component of the induced toroidal dipole moment $T_z$ oriented along the axis of the metamolecule (*z* axis), whereas its net magnetic dipole and quadrupole moments are negligible.

The qualitative arguments produced above are fully supported by our calculations performed using a full three-dimensional Maxwell equations solver based on the finite element method. We modeled the interaction of the metamaterial array with a linearly polarized wave in the spectral range from 14.5 to 17.0 GHz. Calculated densities of the induced electrical currents were used to compute scattered powers of the resulting conventional magnetic and charge multipoles, as well as the toroidal dipole of the metamolecule (Fig. 3C) (*22*).

The strongest contribution to the metamaterial response at resonance ***I*** is provided by the *y*-component of the magnetic dipole moment $M_y$. Here it radiates more strongly than the electric quadrupole moment by a factor of ~5, and more strongly than the dominant radiating component of the electric dipole $P_z$ and the magnetic quadrupole by several orders of magnitude. Its resonant excitation manifests itself as a peak in reflection and deep in transmission at ~16.1 GHz, with a quality factor *Q* of ~80 (Fig. 3, A and B). The nature of the resonance is illustrated in Fig. 3D, where we plot the distribution of the magnetic field lines in the vicinity of the metamolecule. It shows that the field lines are split in two bundles as they thread the wire loops of the metamolecule, and rejoin immediately outside the structure running along the magnetic field of the incident wave. Such a field line configuration indicates strong coupling of the magnetic dipole mode to the free space, thus explaining the moderate value of the *Q* factor.

Resonance ***II*** is located at ~15.4 GHz and is also seen as a peak in reflection and dip in transmission, but with the *Q* factor reaching 240 (Fig. 3, A and B). Magnetic dipole and electric quadrupole excitations of the metamolecule are not resonant at this frequency. Moreover, here the scattering efficiency of electric and magnetic multipoles, which is directly related to the metamaterial's reflectivity, is low. Therefore, the conventional multipole excitations cannot be responsible for the resonance feature at 15.4 GHz. This indicates that the resonance may be due to a toroidal dipole, which scatters more strongly than any of the conventional multipoles by almost two orders of magnitude (Fig. 3C). The toroidal nature of this excitation is illustrated in Fig. 3E, where the calculated lines of the local magnetic field are seen to form closed loops that are largely confined within the metamolecule (as in a true toroidal coil), giving rise to the *z*-component of the toroidal dipole moment $T_z$. The higher *Q* factor of this mode (in comparison with the magnetic di-

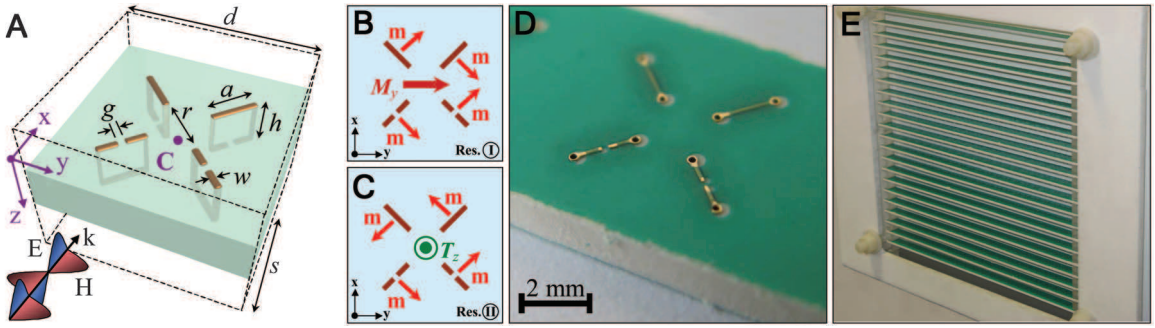


**Fig. 2.** Electromagnetic metamaterial supporting toroidal dipolar excitation. (**A**) Unit cell of the metamaterial, containing four split wire loops embedded into a dielectric slab. (**B** and **C**) Two distinctively different modes of excitation corresponding to magnetic (***I***) and toroidal (***II***) dipole resonances, respectively. (**D**) Close-up photograph of the wire structure of the toroidal metamolecule. (**E**) Assembled metamaterial slab, 8 mm × 176 mm × 165 mm (green solder resist was removed before the measurements).

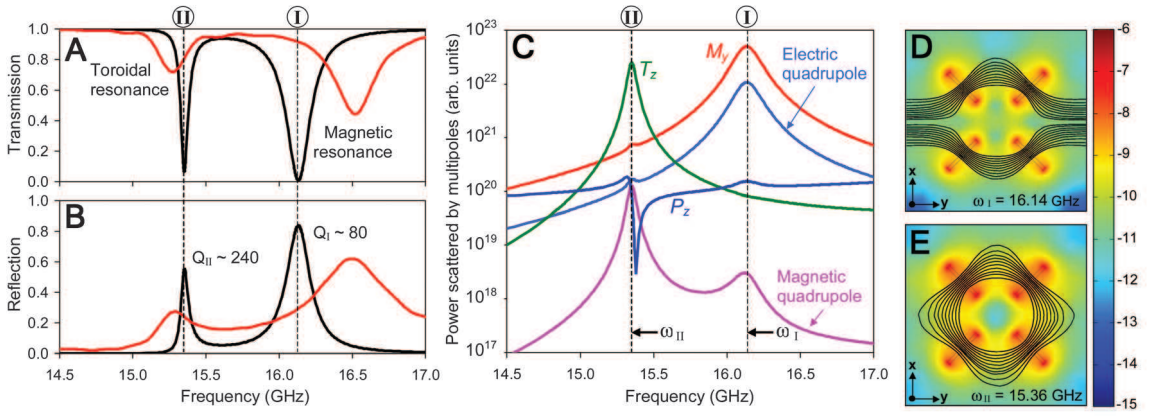


**Fig. 3.** Resonant toroidal response of the metamaterial. (**A** and **B**) Calculated (black lines) and measured (red lines) transmission and reflection spectra of the metamaterial. Positions of the calculated magnetic and toroidal dipole resonances, ***I*** and ***II***, are marked by vertical dashed lines. (**C**) Dispersion of scattered power for various multipole moments induced in the metamolecule that contribute to the reflection and transmission spectra of the metamaterial slab. (**D** and **E**) Distributions of magnetic field lines for correspondingly magnetic (***I***) and toroidal (***II***) dipole resonances plotted over the color maps of the magnetic energy density (logarithmic scale).

pole mode $\boldsymbol{I}$) is the direct consequence of its strong confinement and weak free-space coupling. Note that at the toroidal resonance, the electrical dipole excitation has a strong net $x$-component $P_x$, which results from the presence of the splits in the loops of the metamolecule. However, as $P_x$ oscillates along the wave propagation direction, it does not contribute to the metamaterial's reflection and transmission.

We observed the toroidal dipole resonance experimentally in a metamaterial slab formed by a 22 × 22 array of toroidal metamolecules (Fig. 2D). The rows of the array were manufactured from metalized microwave laminate strips by high-resolution printed board technology; these rows were than stacked at a regular interval with the axes of the metamolecules aligned in the plane of the array (Fig. 2E). The transmission and reflection spectra of the slab were measured in an anechoic chamber by means of a vector network analyzer and linearly polarized horn antennas (*22*). The experimental data (Fig. 3, A and B) show good agreement with the simulated spectra. The somewhat lower $Q$ factors of the measured resonances are attributed to the manufacturing tolerance and limited size of the metamaterial array, as well as to some divergence of the wave front of the incident microwave beam. The slight mismatch between the calculated and measured values of the resonance frequencies (0.7% and 2% for the corresponding toroidal and magnetic resonances, respectively) is due to the limitations of the fabrication process (*22*), which did not allow perfect replication of the design features, such as the profile of the wires forming the loops; this could affect the wires' inductance and intramolecular interactions.

Toroidal multipoles are routinely neglected in the constitutive relations, boundary conditions, electromagnetic forces, and calculation of momentum loss and radiation intensity of charge-current configurations (*5*, *23*–*25*). Our results provide compelling evidence of a resonant response that can only be attributed to a toroidal dipole excitation of the metamaterial structure in the microwave part of the spectrum. Downsizing the structure should allow observation of a plasmonic toroidal mode at optical frequencies in a single submicrometer metallic toroid, as well as in arrays of such toroids. Molecular systems such as fullerene rings are also predicted to support toroidal moments (*6*), thus urging the development of a quantum mechanical description of the light-matter interaction with toroidal molecular structures. Moreover, our results call for the development of a deeper understanding of the quantum mechanism of intramolecular interactions involving toroidal molecular structures, which are widespread in nature.

### References and Notes


1. J. D. Jackson, *Classical Electrodynamics* (Wiley, New York, ed. 3, 1999), chap. 16.
2. L. D. Landau, E. M. Lifschitz, *Course of Theoretical Physics* (Pergamon, New York, ed. 4, 1993), vol. 2.
3. Ia. B. Zel'dovich, *Sov. Phys. JETP* **6**, 1184 (1958).
4. W. C. Haxton, *Science* **275**, 1753 (1997).
5. E. E. Radescu, G. Vaman, *Phys. Rev. E* **65**, 046609 (2002).
6. A. Ceulemans, L. F. Chibotaru, P. Fowler, *Phys. Rev. Lett.* **80**, 1861 (1998).
7. I. I. Naumov, L. Bellaiche, H. Fu, *Nature* **432**, 737 (2004).
8. V. M. Dubovik, L. A. Tosunyan, V. V. Tugushev, *Sov. Phys. JETP* **63**, 344 (1986).
9. G. N. Afanasiev, V. M. Dubovik, *Phys. Part. Nucl.* **29**, 366 (1998).
10. A. D. Boardman, K. Marinov, N. Zheludev, V. A. Fedotov, *Phys. Rev. E* **72**, 036603 (2005).
11. N. Papasimakis, V. A. Fedotov, K. Marinov, N. I. Zheludev, *Phys. Rev. Lett.* **103**, 093901 (2009).
12. K. Marinov, A. D. Boardman, V. A. Fedotov, N. Zheludev, *N. J. Phys.* **9**, 324 (2007).
13. G. N. Afanasiev, *J. Phys. D* **34**, 539 (2001).
14. K. Sawada, N. Nagaosa, *Phys. Rev. Lett.* **95**, 237402 (2005).
15. V. M. Dubovik, V. V. Tugushev, *Phys. Rep.* **187**, 145 (1990).
16. V. M. Dubovik, A. A. Cheshkov, *Sov. J. Part. Nucl.* **5**, 318 (1974).
17. G. N. Afanasiev, V. M. Dubovik, *J. Phys. A* **25**, 4869 (1992).
18. A. Góngora T., E. Ley-Koo, *Rev. Mex. Fis. E* **52**, 188 (2006).
19. V. A. Fedotov, K. Marinov, A. D. Boardman, N. I. Zheludev, *N. J. Phys.* **9**, 95 (2007).
20. S. Alborghetti *et al.*, *N. J. Phys.* **10**, 063019 (2008).
21. D. R. Smith, J. B. Pendry, M. C. K. Wiltshire, *Science* **305**, 788 (2004).
22. See supporting material on *Science* Online.
23. E. V. Tkalya, *Phys. Rev. A* **65**, 022504 (2002).
24. V. M. Dubovik, M. A. Martsenyuk, B. Saha, *Phys. Rev. E* **61**, 7087 (2000).
25. H. Schmid, *Ferroelectrics* **252**, 41 (2001).


26. Supported by the UK Engineering and Physical Sciences Research Council, the Royal Society, and the Leverhulme Trust.


### Supporting Online Material

www.sciencemag.org/cgi/content/full/science.1197172/DC1
Materials and Methods
Fig. S1
References

31 August 2010; accepted 19 October 2010
Published online 4 November 2010;
10.1126/science.1197172

# Evidence of Supersolidity in Rotating Solid Helium

**H. Choi,[1] D. Takahashi,[2] K. Kono,[2] E. Kim[1]***

**Supersolidity, the appearance of zero-viscosity flow in solids, was first indicated in helium-4 torsional oscillator (TO) experiments. In this apparatus, the irrotationality of the superfluid component causes it to decouple from the underlying normal solid, leading to a reduction in the resonant period of the TO. However, the resonant period may be altered for reasons other than supersolidity, such as the temperature dependence of the elastic modulus of solid helium. Superimposing rotation onto oscillatory measurements may distinguish between supersolidity and classical effects. We performed such simultaneous measurements of the TO and the shear modulus, and observed substantial change in the resonant period with rotational speed where the modulus remained unchanged. This contrasting behavior suggests that the decrease in the TO period is a result of supersolidity.**

Because of its irrotational nature, a superfluid decouples from its container when subject to rotation, leading to a reduction of rotational inertia at the superfluid transition. The missing rotational inertia is referred to as nonclassical rotation inertia (NCRI) (*1*). In addition to the fluid $^4$He, the reduction of the resonant period of a torsional oscillator (TO) was also found in solid $^4$He and was interpreted as a manifestation of a paradoxical state of matter: supersolidity (*2*, *3*).

Since the initial discovery, a number of puzzles have arisen, such as the lack of a critical exponent at the transition, extremely low critical velocity (*2*–*4*), dc flow that depends on experimental conditions (*5*–*11*), and lack of the second or fourth sound (*12*, *13*). Without direct evidence of phase coherence in solid $^4$He, a different interpretation of TO experiments is possible (*14*–*16*). In a perfectly rigid solid, all parts of the solid oscillate perfectly in phase with the torsional cell. The resonant frequency $\omega_0$ of an ideal TO is directly related to $I$, the moment of inertia of the torsion bob, and is described by $\omega_0 = \sqrt{K/I}$, where $K$ is the spring constant of the torsion rod. For a viscoelastic solid, on the other hand, parts of the solid could lag behind the cell and build stress within the solid. As a consequence, the resonant period shift may not be affected by the change in rotational inertia only, but may also reflect a change in the temperature-dependent viscoelasticity of the solid. In oscillatory experiments, the resonant period can therefore change without invoking supersolidity.

This scenario is supported by a marked resemblance between the TO and shear modulus measurements (*17*). However, estimates of the viscoelastic effects based on the magnitude of the measured shear modulus change do not fully account for the size of the period change observed in TO measurements. This inconsistency has partially inspired alternative compound models such as the superglass (*18*).

A more recent phenomenological model that includes a contribution from the additional strain originating from sliding dislocations (*19*) was also

[1]Department of Physics and Center for Supersolid and Quantum Matter Research, KAIST, Daejeon 305-701, Republic of Korea. [2]Low Temperature Physics Laboratory, RIKEN, Wakoshi, Saitama 351-0198, Japan.

*To whom correspondence should be addressed. E-mail: eunseong@kaist.edu